

# Synergistic Photoprotection: Enhanced Stability of Vulpinic Acid through Interaction with Exocellular Polysaccharides

Tanzil Mahmud,<sup>†§κ</sup> Derek C. Moore,<sup>§κ</sup> Ilya D. Dergachev,<sup>§κ</sup> Henry Sun,<sup>∞</sup> Sergey A. Varganov,<sup>§\*</sup>

Matthew J. Tucker,<sup>†§\*</sup> Christopher S. Jeffrey<sup>†§\*</sup>

§ Department of Chemistry, University of Nevada, Reno, Reno, NV 89557

∞Desert Research Institute, Las Vegas, NV 89119

† Hitchcock Center for Chemical—Ecology, University of Nevada at Reno, Reno, NV 89557

<sup>κ</sup>authors contributed equally

\*indicates co-corresponding authors:

Christopher S. Jeffrey, [cjeffrey@unr.edu](mailto:cjeffrey@unr.edu); Matthew J. Tucker, [matthewtucker@unr.edu](mailto:matthewtucker@unr.edu); Sergey A. Varganov, [svarganov@unr.edu](mailto:svarganov@unr.edu)

KEYWORDS: UV-Protection, lichen pigments, photostability

## Abstract

Lichens have been of great interest in exobiological studies due to their remarkable tolerance to ultraviolet (UV) radiation. These organisms employ extracellular pigments for screening high-energy solar radiation, allowing the photosynthetically active radiation to pass through and be utilized by the photosymbiont. These pigments are found co-occurring within polysaccharide scaffolds in the lichen

cortex. Despite extensive studies on isolated lichen pigments, the potential role of exopolysaccharides (EPS) in the photoprotective system of lichens has remained unclear. We report detailed photophysical studies on the wolf lichen pigment vulpinic acid in pullulan, a polysaccharide that mimics lichen EPS. Solid phase studies demonstrate that the pigment's photostability is greatly enhanced in the pullulan polysaccharide matrix. Analysis of ultrafast transient absorption infrared spectroscopy indicates potential interactions of the polysaccharide inhibiting the relaxation pathway of vulpinic acid upon UV photoexcitation. These polysaccharides interrupt an intramolecular proton transfer that traditionally leads to photodecomposition of the isolated vulpinic acid compound. These results suggest a crucial role of EPS in the photoprotective systems of lichens. The interaction between vulpinic acid and pullulan exemplifies a non-spectator role of polysaccharides in photoprotection, potentially contributing to the extraordinary resilience of lichens and cyanobacteria. This polysaccharide-pigment interaction may represent a general strategy among extremophiles to mitigate UV-induced damage, highlighting the importance of interdisciplinary approaches in unraveling complex biological systems.

## Introduction

Protection from excessive solar radiation—broadly termed photoprotection—is relevant for any lifeform that is exposed to sunlight. It is especially important for photosynthetic organisms as they inevitably need to harvest solar radiation while experiencing diurnal and annual variations in solar irradiance. Among several photoprotective strategies found in nature, optical screening-based photoprotection is a hallmark of photosynthetic organisms as screening pigments are ubiquitously found in them.<sup>1</sup> Such photoprotective systems employ screening pigments as an optical filter to prevent high energy UV radiation from entering the cell.<sup>2</sup> Lichens—the symbiotic association between fungi and algae or cyanobacteria—are some of the most stress tolerant organisms on Earth and exhibit the extreme form of this photoprotection. Lichens synthesize a wide array of UV screening compounds and can accumulate very high quantities of sunscreen pigments in their outer cortex.<sup>3,4</sup> These cortical lichen pigments play a

major role in the superior UV tolerance in lichens.<sup>3, 4</sup> This, along with desiccation and photooxidative damage tolerance, has made lichens model organisms for studying survivability in outer space and early Earth-like conditions.<sup>5-7</sup>

A notable aspect of lichen UV screening pigments is their localization in the outer cortex along with polysaccharides.<sup>8, 9</sup> Although this polysaccharide matrix is known to play a role in desiccation tolerance in these organisms,<sup>10</sup> its potential involvement in lichen photoprotection has not been studied. Coexistence of UV absorbing pigments and polysaccharides in the lichen cortex provides a strong reason for such an investigation (Figure 1). Polysaccharides are expected to provide hydrogen bonding interaction to the pigment molecules. Such interactions have been shown to affect the stability of DNA and its ability to dissipate UV energy efficiently through double hydrogen transfer between the guanidine-cytosine base pair,<sup>11, 12</sup> suggesting that cortex polysaccharide may play a role in lichen photoprotection.

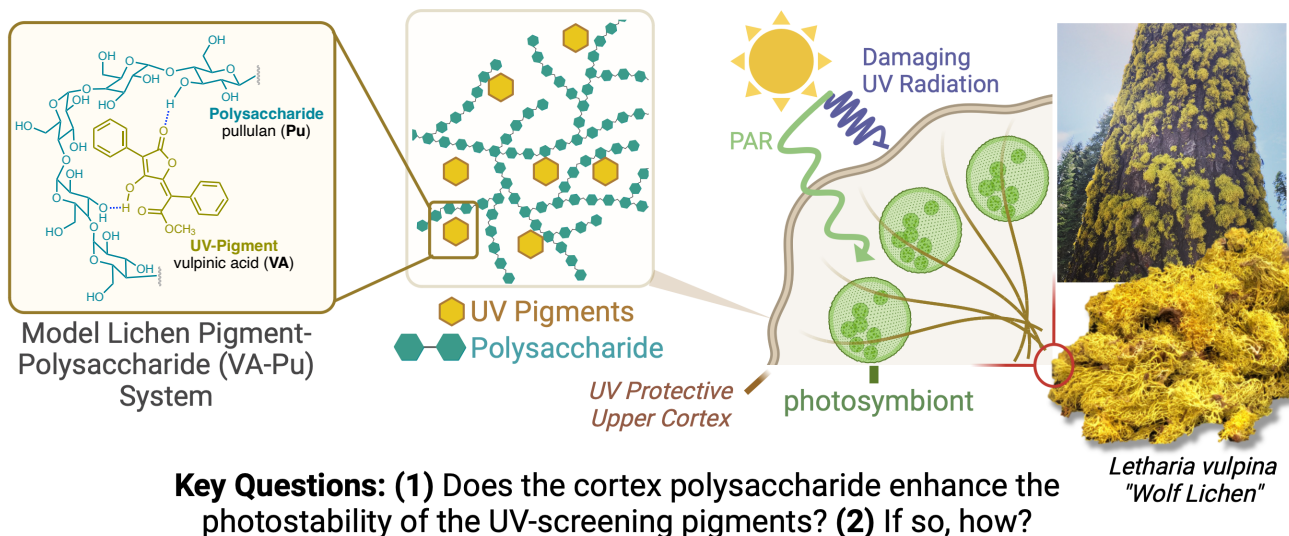


**Figure 1:** A general schematic illustrating the outer cortex pigments imbedded in a polysaccharide matrix as a synergistic photoprotective system explaining the extreme ability for lichen to survive under exposure to intense UV radiation.

We report *in vitro* studies on vulpinic acid (VA), the major UV absorbing pigment in *Letharia vulpina*, in a biomimetic polysaccharide matrix to investigate the role of the cortex polysaccharides in lichen photoprotection. Vulpinic acid has been established as a nonfluorescent UV and blue-light screening

photoprotectant.<sup>13, 14,15</sup> The fungal polysaccharide pullulan (**Pu**) was utilized to mimic lichen cortex polysaccharide environment. Solid phase photostability studies on VA-pullulan (**VA-Pu**) composite films showed a remarkable enhancement in photostability compared to isolated pigment films, implying that the polysaccharide is possibly an active component of the lichen exocellular photoprotective system. Ultrafast transient absorption IR spectroscopy was performed to elucidate the nature of the **VA-Pu** interaction on short timescales. The results showed direct involvement of the polysaccharide in the excited-state processes of **VA**. We employed density functional theory (DFT) and time-dependent density functional theory (TD-DFT) calculations to evaluate the photochemical consequences and excited state features of **VA** and **VA-Pu** systems. Based on these investigations, a mechanistic hypothesis is presented where phototautomerism of vulpinic acid is discussed in the presence and absence of a polysaccharide. The hydrogen bonding network and proton-rich environment of the polysaccharide matrix is strongly implicated in the photostability enhancement of vulpinic acid in pullulan. Studying such synergistic interactions will help us understand biological processes in early-Earth conditions and guide us in exobiological studies.

## Results and discussion

### Enhancement of Vulpinic acid Photostability in a Polysaccharide Matrix

Solid phase photostability studies were performed on vulpinic acid (**VA**) in distinct chemical environments to uncover different photophysical aspects of light screening by the cortical lichen pigment. To investigate the role of exopolysaccharides in the photoprotective activity of vulpinic acid, its photostability was tested in three different forms: isolated vulpinic acid (**VA**), vulpinic acid in  $\beta$ -cyclodextrin complex (**VA- $\beta$ -CD**), and vulpinic acid-pullulan composite (**VA-Pu**). All studies were performed in solid phase to better mimic the extracellular photoprotective system in lichens. The vulpinic acid in  $\beta$ -cyclodextrin encapsulation complex was expected to eliminate bimolecular interaction of

vulpinic acid molecules and provide a physical environment similar to a polysaccharide. Finally, a composite film consisting of vulpinic acid crystals dispersed in the fungal polysaccharide pullulan was utilized to mimic the physical and chemical environment in a lichen cortex.

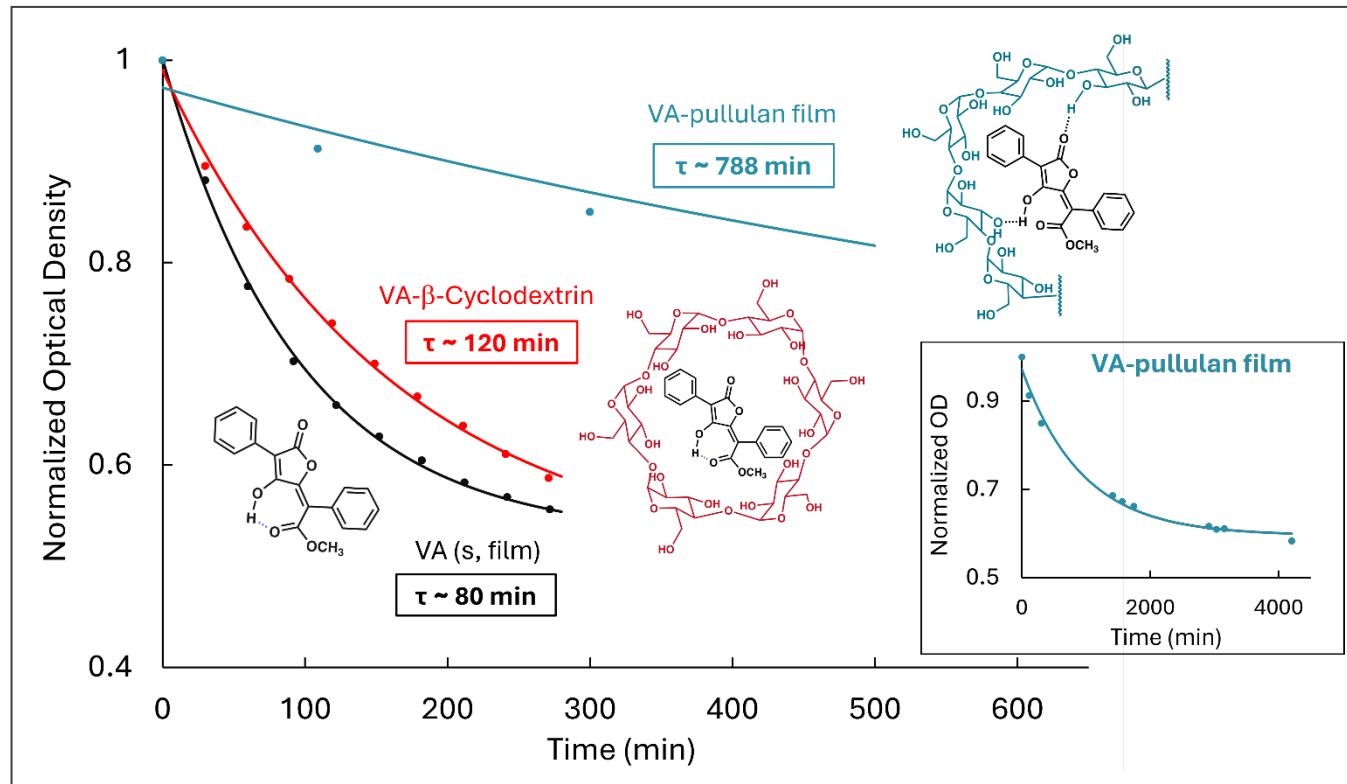


**Figure 2:** Photodegradation curves of vulpinic acid (black), vulpinic acid- $\beta$ -cyclodextrin complex (red) and vulpinic acid-pullulan composite film (blue) along with fits of time constants of decay,  $\tau$  from their single exponential fit of the form  $y = Ae^{-x/\tau} + y_0$ . The photodegradation curve for VA-pullulan film over an extended timescale is shown in the inset.

Thin films of each of these samples were irradiated at 400 nm and changes in their optical densities were periodically measured at 400 nm (see UV-Vis spectra in Figure S1).  $\beta$ -cyclodextrin and pullulan are both transparent in this wavelength range. The decays are fit to a single exponential to extract a time constant  $\tau$  for each system (Figure 2). These time constants indicate the rate of degradation of the pigment in each system and hence is a measure of photostability of the pigment. The values of these time constants are  $79.71 \pm 22.57$  (VA),  $120.09 \pm 58.21$  (VA- $\beta$ -CD), and  $787.81 \pm 211.36$  (VA-Pu) in minutes. The largest contribution to the standard deviation in the measurements arises due to the unevenness of the film

distribution on the quartz plate. The higher time constants indicate slower rates of pigment degradation. To account for any differences in the power of the irradiation source, the time constants were expressed as decay constants with units of total number of incident photons (shown in Figures S2). **VA- $\beta$ -CD** showed a 50% enhancement in photostability compared to isolated **VA**.  $\beta$ -cyclodextrin encapsulation has been found to enhance the photostability of various sunscreen pigments.<sup>16-19</sup> Encapsulated **VA** molecules are expected to undergo unimolecular photodegradation processes, so the overall enhancement of the decay time of **VA- $\beta$ -CD** is likely a result of  $\beta$ -cyclodextrin providing a competing vibrational relaxation scaffold to excited state of VA molecules assuming **VA** and **VA- $\beta$ -CD** have similar mechanisms of dissipation. The decay time of vulpinic acid in a pullulan composite film (**VA-Pu**) was found to be an order of magnitude higher than the isolated VA film. This signifies that photodegradation of vulpinic acid in pullulan happens at a rate an order of magnitude lower compared to its isolated crystalline form. Overall, these results illustrate that the degradation times are significantly influenced by interactions between the pigment and its local chemical environment, accentuating the involvement of the polysaccharide matrix in UV protection of lichen organisms. In particular, the local environment acts as a much larger scaffold for energy dissipation via vibrational relaxation.

## **FTIR and DFT calculations suggest phototautomerism of vulpinic acid as a major photochemical outcome**

Photodegradation of **VA** films upon long-term irradiation at 400 nm was monitored by periodically collecting FTIR spectra of the samples to probe structural changes associated with the degradation. Changes in peak intensities and the emergence of new IR peaks provide insights into the structural changes induced in **VA** upon irradiation. Decreasing peak intensities were observed in **VA** at  $1598\text{ cm}^{-1}$ ,  $1612\text{ cm}^{-1}$ ,  $1678\text{ cm}^{-1}$ , and  $1774\text{ cm}^{-1}$  (Figure 3). A broad increase was observed between approximately  $1685\text{ cm}^{-1}$  and  $1755\text{ cm}^{-1}$ , which indicates a distribution of multiple products forms upon long-term irradiation. To interpret the differences between initial and final FTIR spectra, DFT calculations were performed at

B3LYP/def2-SVPD level to compute the geometry and the ground state FTIR spectra. Of the major isomers of vulpinic acid, **VA-T<sub>1</sub>** was established as the ground state structure by single-crystal X-ray diffraction (scXRD) of vulpinic acid isolated from *Letharia vulpina* (Figure 3, Panel B). We found excellent agreement between the experimental and computed geometries as well as between the FTIR spectra and DFT calculations, where the **VA-T<sub>1</sub>** isomer was also found to be the lowest energy isomer (Figure 3, Panel B). When selecting likely photoproducts to evaluate with computational studies, tautomers and *E/Z*-isomers of each tautomer of VA were considered. Of these, only *E* isomer of **VA-T<sub>2</sub>** and the 1,3-dicarbonyl tautomer (**VA-CT**) strongly resembled the experimental observations (Figure S7). **VA-T<sub>2</sub>** showed emergence of absorption between 1690 cm<sup>-1</sup> and 1760 cm<sup>-1</sup> and an overall decrease in peak intensities in the 1500-1680 cm<sup>-1</sup> range when compared to **VA-T<sub>1</sub>** spectrum, supporting that the **VA-T<sub>2</sub>** isomer of vulpinic acid is a major photoproduct of vulpinic acid in the solid phase upon continuous irradiation.

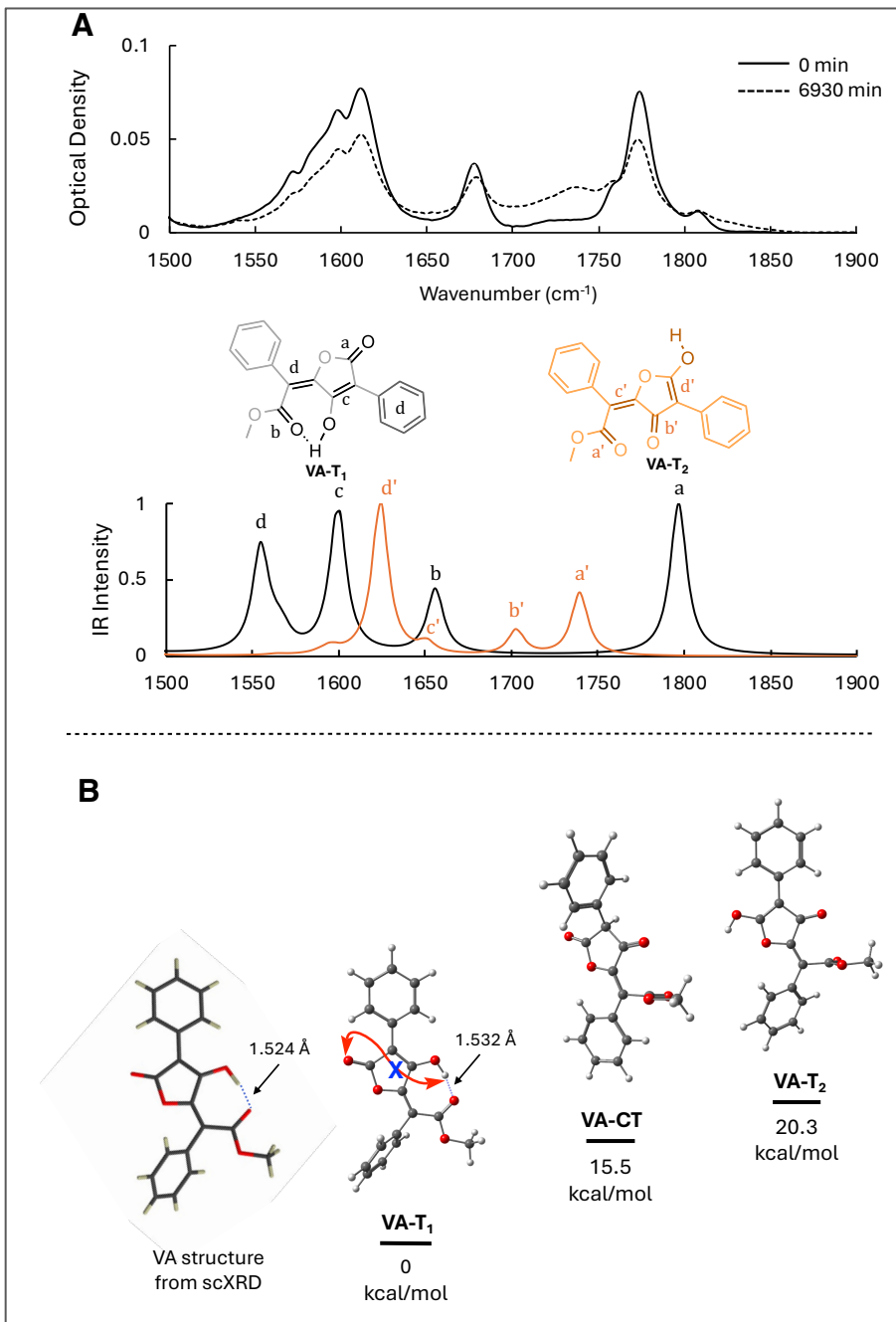


**Figure 3:** Top: Steady-state FTIR spectra recorded over the time of UV exposure of a neat VA film and DFT calculated FTIR spectra for the **VA-T<sub>1</sub>** and **VA-T<sub>2</sub>** isomers indicating clear overlap with vibrational frequencies observed upon prolonged irradiation with UV (400 nm). Bottom: Likely tautomerization of the thermodynamically dominant **VA-T<sub>1</sub>** tautomer to the thermodynamically less stable **VA-T<sub>2</sub>** tautomer with an arrow indicating the geometrically restricted intramolecular proton transfer linking the two forms.

Because conformational change is expected to be hindered in solid phase, keto-enol tautomerization between **VA-T<sub>1</sub>** and **VA-T<sub>2</sub>** may be favored as a relaxation mechanism as it requires

minimal change in the molecular geometry. However, it is unlikely to happen through a single-step unimolecular process in vulpinic acid due to unfavorable geometry for a proton transfer from the enol OH to the lactone carbonyl (Figure 3). Solvent-assisted proton transfer between the two centers may be possible. In the absence of solvent-mediated interactions, it is reasonable to assume that tautomerization of VA happens through a more complex, multi-step process; presumably through formation of one or more intermediates, such as the C-tautomer (VA-CT).<sup>20, 21</sup>

FTIR photodegradation studies were also performed on a **VA-Pu** film, which showed similar spectral changes upon irradiation (Figure S3). The **VA-Pu** system was modeled in DFT calculations by placing two methanol molecules on either side of a **VA** molecule, providing relevant hydrogen-bonding interactions (Figure S6). The similarities in spectral features between these two systems (Figure 3 and Figure S3) suggest that VA forms same/similar photoproducts in presence or absence of pullulan. The vastly different time constants of decay in the photodegradation studies (Figure 2) indicate that the products form at different rates, signifying involvement of different photochemical steps/processes between the two systems (or similar processes happening at slower rates).

### **Transient Absorption IR spectroscopy and TD-DFT calculations reveal excited-state features and key differences in relaxation pathway of VA in polysaccharide**

Since photoexcited processes typically unfold within picosecond or even shorter timescales, theoretical investigations utilizing electronic structure computations are indispensable for elucidating the comprehensive mechanism, which often involves several relaxation pathways.<sup>22-25</sup> The dynamics of the vulpinic acid and VA-pullulan systems on short (picosecond) timescales were evaluated using transient absorption spectroscopy and TD-DFT calculations. Our transient absorption IR experiments highlighted significant changes in kinetic traces of the transient spectra, revealing differences in the excitation-relaxation mechanisms of **VA** (Figure 4, Panel A) and **VA-Pu** composite film (Figure 4, Panel B). The

combination of a 400 nm pump pulse and broadband IR probe pulse allowed for the examination of the excited-state IR spectrum between 1500-1750 cm<sup>-1</sup> at delay times ranging from a hundred femtoseconds to 3 nanoseconds. Several absorption and bleach signals appear shortly after time zero in each of the systems. Some of the prominent signals that appear in both **VA** and **VA-Pu** include the transient absorptions near 1716 cm<sup>-1</sup> and 1575 cm<sup>-1</sup>, and the bleach around 1600 cm<sup>-1</sup> (Figure 4, Panels A and B). A comparison of the transient absorption spectrum at 2 ps and steady-state difference FTIR spectrum (spectrum before irradiation subtracted from spectrum after irradiation) is provided for both **VA** and **VA-Pu** in Figure S4. As shown, there is little overlap between the short-timescale transient and the long timescale FTIR difference spectra. These results suggest the presence of photochemical processes which lead to intermediate structures that are not present in the final photoproducts, i.e. long-lived intermediates, which may include structures resembling the various tautomers of **VA**.

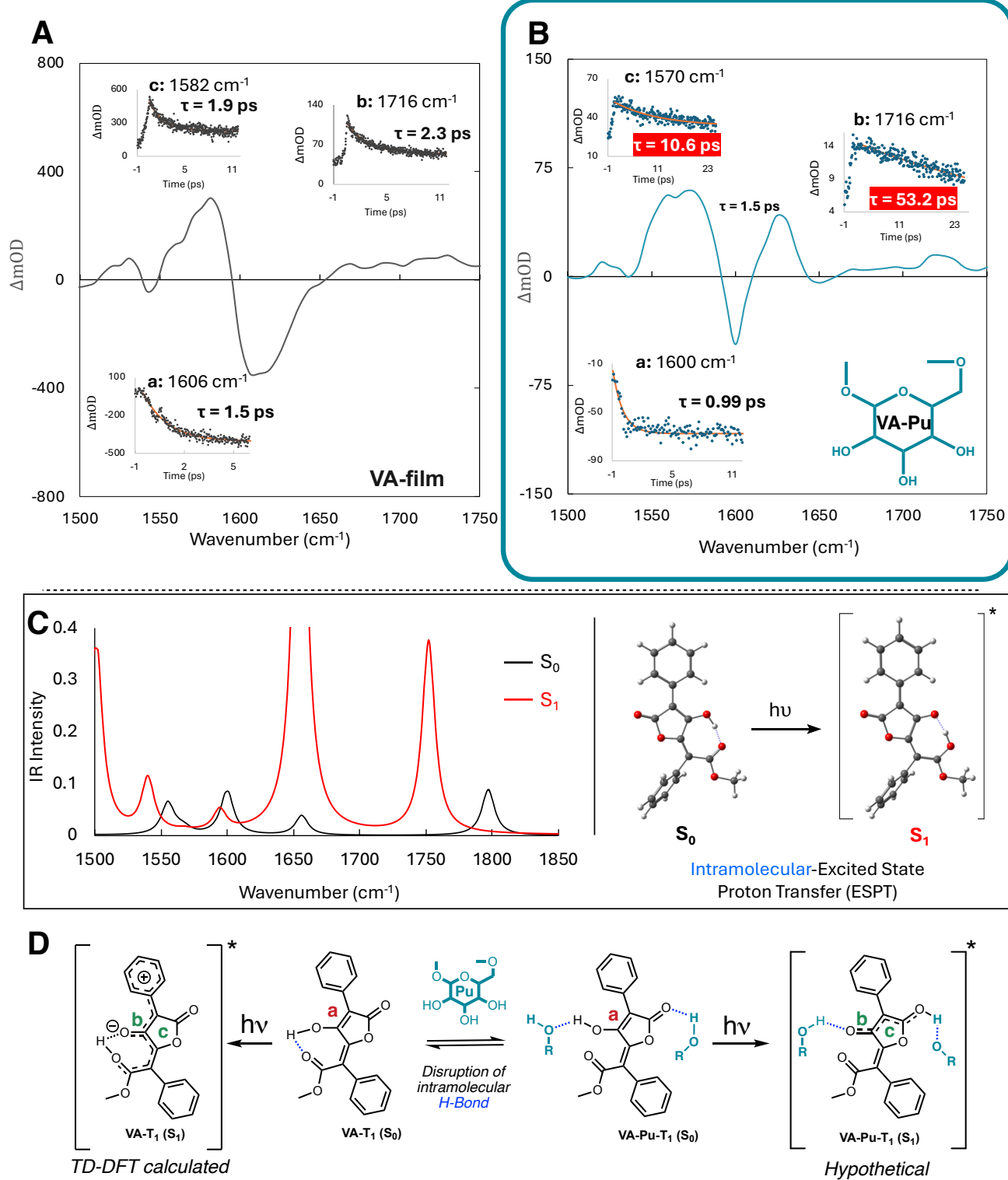


**Figure 4:** Transient difference spectra of solid **VA** film (Panel A) and **VA-Pu** composite film (Panel B) at 2 ps with structural annotation of vibrational bleaching and species development. Kinetic traces of important spectral regions are shown on the insets with corresponding frequencies. Time constants,  $\tau$ , are extracted from their single exponential fit,  $y = Ae^{-x/\tau} + y_0$  and indicate greatly extended decay constants for the **VA-Pu** system. **Panel C:** TD-DFT computed spectra of ground state ( $S_0$ , black) and the first excited state ( $S_1$ , red). The spectral features are in

agreement with the transient absorption spectra from experiments. The calculated optimized geometries suggest an excited-state intramolecular proton transfer event in vulpinic acid upon excitation (right). **Panel D:** Tentatively assigned structural changes observed on the picosecond timescale that are supported by TD-DFT calculations indicating the relevance of a proton transfer event in both **VA** and **VA-Pu**.

Examining the kinetic traces of prominent signals in the transient absorption spectra reveals specific structural rearrangements occurring upon irradiation. TD-DFT calculations of the excited state of the **VA-T<sub>1</sub>** isomer support that the bleach signal at 1598 cm<sup>-1</sup> for **VA** represents the alkene of the butenolide resulting from the initial intramolecular-excited state proton transfer (ESPT) to the ester carbonyl, occurring with a time constant of 1.5 ps (Figure 4). The traces of two positive-going signals (1582 cm<sup>-1</sup> and 1716 cm<sup>-1</sup>) represent the subsequent intermediate steps within the intramolecular-ESPT. The 1582 cm<sup>-1</sup> decaying signal (~1.9 ps) corresponds to the formation of an excited state ( $S_1$ ) intermediate while the 1716 cm<sup>-1</sup> decaying signal (~2.3 ps) represents the formation of the carbonyl (Figure 4) upon further migration of the proton. The bleach signal at 1600 cm<sup>-1</sup> persists for longer than 3 ns without decaying (Figure S5). All signals reach their largest magnitudes in approximately 0.5-1 picoseconds, which is around the timescale corresponding to a typical intramolecular proton transfer.<sup>26,27</sup>

Both systems show broadly similar transient absorption signal changes with the major differences being in the time constants of the kinetic traces observed at ~1575 cm<sup>-1</sup> and 1716 cm<sup>-1</sup>, suggesting differences in their excited-state intermediate lifetimes and relaxation pathways (Figure 4). For the **VA-Pu** positive signal at 1570 cm<sup>-1</sup> the time constant is 10.6 ps, which is five times larger than that for the analogous peak in **VA** (Figure 4, Panel B). A more drastic difference is observed for the absorption at 1716 cm<sup>-1</sup>. The time constant for this decaying signal is 53.2 ps, which is over twenty times larger than the time constant at this frequency for **VA**. These significant increases in the time constants strongly suggest the involvement of pullulan in kinetic trapping along the relaxation pathway of the excited state of **VA**, inhibiting the pathways associated with intermediate structure through external hydrogen bonding that interrupts the intramolecular hydrogen bond in **VA-T<sub>1</sub>**.

## Conclusion and overall mechanistic scheme

Our study presents compelling evidence for the active participation of polysaccharides in the photoprotection system of lichens, as demonstrated by the significant enhancement of vulpinic acid (**VA**) photostability in a pullulan matrix. The observed ~10-fold increase in photostability of **VA** in the pullulan composite film compared to isolated VA emphasizes the non-spectator role of the polysaccharide in the photophysical processes and photostability of the pigment. Transient absorption infrared spectroscopy, coupled with DFT and TD-DFT computational studies, reveals key differences in potential relaxation pathways of **VA** when embedded in a polysaccharide matrix that underscore the observed dramatic increase in photostability of **VA** in a pullulan film. As a neat film of **VA**, computational and transient absorption IR methods support an intramolecular-ESPT from the enol to the methyl ester. In other established sunscreen systems, such as benzophenones and hydroxyanthroquinones, the intramolecular-ESPT followed by relaxation to a tautomeric form has been established as the main mode of radiationless decay to the ground state.<sup>28-35</sup> However, in the case of **VA**, there are significant geometric impediments to relaxing to the other stable tautomeric products (**VA-T<sub>2</sub>** and **VA-CT**) through a proton transfer event and would require external proton donors or acceptors to complete this proton transfer. It is likely that the highly reactive excited state provides a significant source of degradation through participating in irreversible reactions in the neat **VA** film. However, in the presence of the polysaccharide pullulan, this pathway can be interrupted, allowing for efficient tautomerization to the **VA-T<sub>2</sub>** isomer either after intramolecular ESPT or through an intermolecular ESPT.<sup>36-39</sup> While the limitations of our computational approaches prevent the accurate modeling of the excited state of the **VA** imbedded in pullulan, computational evaluation of **VA** with two discrete methanol molecules supports that the intramolecular hydrogen bond can be interrupted in the ground state without significant energetic penalties (Figure S6). It is likely to change the intramolecular-ESPT to a transition that is described more as a conformational twist than the proton transfer computed from the TD-DFT calculations of the un-solvated system.<sup>40</sup>

Moreover, comparisons of the lifetimes of key vibrational modes strongly suggests that proton transfer, whether intramolecular or intermolecular, is occurring in both the **VA** and **VA-Pu** films (bleaching at 1600/1606 cm<sup>-1</sup>). However, the relaxation lifetimes and pathways are significantly different, especially with respect to the vibrational mode corresponding to the carbonyl that would be developing upon tautomerization to a structure resembling **VA-T<sub>2</sub>** [**VA** (neat) 1716 cm<sup>-1</sup>  $\tau$  = 2.3 ps vs. **VA-Pu**  $\tau$  = 53.2 ps, Figure 4].

Given these results we propose a mechanistic scheme whereby an excited state proton transfer results from the absorbance of a photon by **VA** (Figure 5). In the case of the neat **VA**, the strong intramolecular hydrogen bond enforces an intramolecular-ESPT to the ester carbonyl.<sup>39, 41</sup> This reactive product most likely relaxes back to the ground state through back proton transfer followed by internal conversion; however, it is susceptible to irreversible photoreactions leading to the observed photodegradation. When **VA** is imbedded in the polysaccharide pullulan (**VA-Pu**), the intramolecular H-bond could be interrupted which upon excitation undergoes an intermolecular proton transfer eventually relaxing to **VA-Pu-T<sub>2</sub>**, which can revert to the thermodynamically favored **VA-Pu-T<sub>1</sub>** tautomer. This efficient photocycle, enabled by the polysaccharide, prevents significant photodegradation that would otherwise occur through the intramolecular-ESPT pathway. The mechanistic insight gained by our results highlights the critical role of exopolysaccharides in the extracellular photoprotective systems of lichens and possibly other extremophiles. By switching the major relaxation pathway from intramolecular-ESPT to intermolecular-ESPT/tautomerization, the polysaccharide matrix not only enhances the photostability of the pigment but also facilitates a sustainable photoprotective cycle. This study thus highlights the evolutionary significance of polysaccharide-pigment interactions in natural photoprotection systems, providing a deeper understanding of the resilience mechanisms in extremophiles and offering potential strategies for developing bio-inspired UV protection solutions.

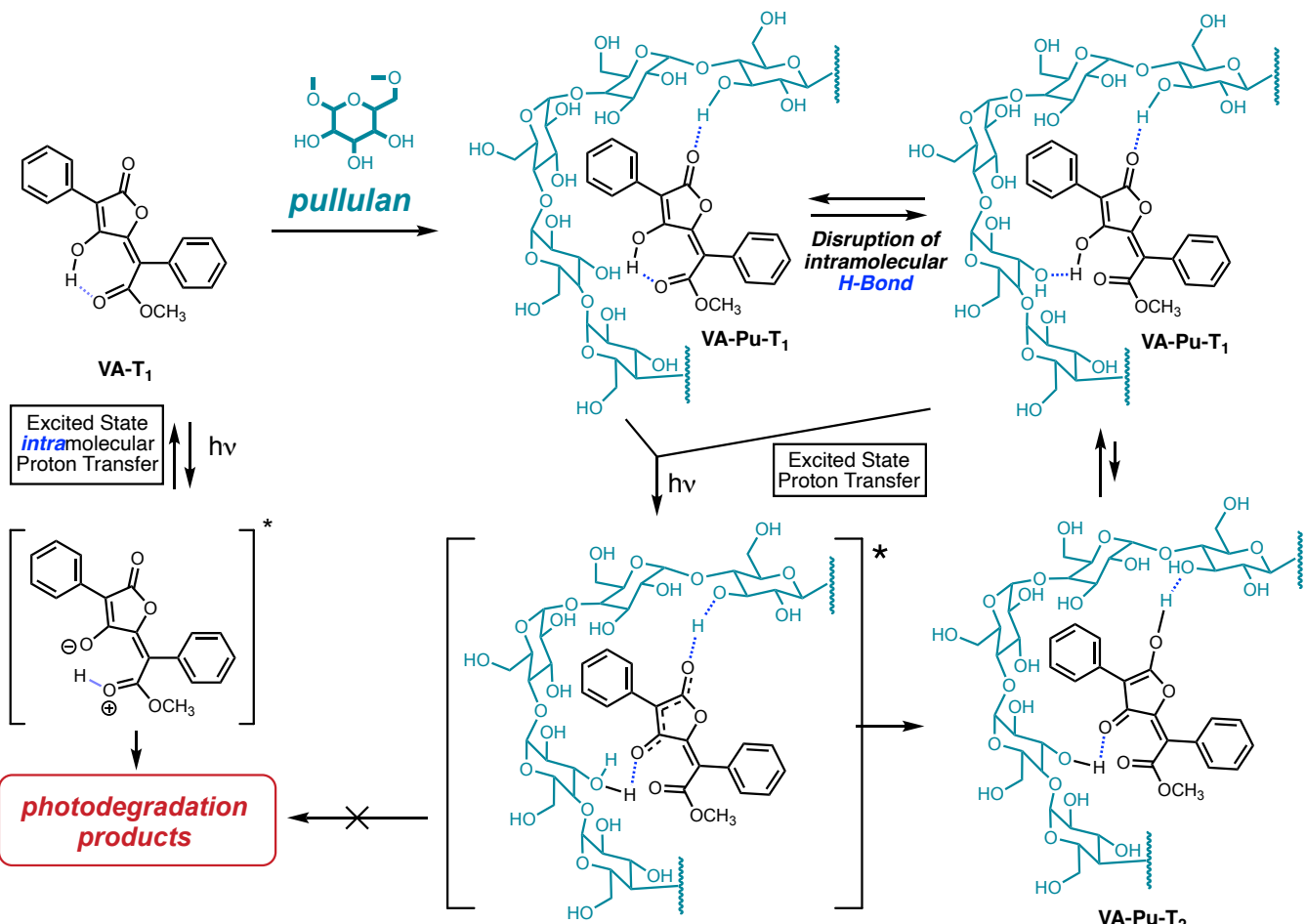


**Figure 5:** Overall mechanistic scheme supported by the results of this study. VA undergoes an intramolecular excited state proton transfer to the ester carbonyl in the absence of an external proton donor-acceptor. The VA-Pu complex can maintain a stabilizing photocycle by interrupting this process and/or quenching the resulting intramolecular excited state proton transfer product leading to rapid conversion to VA-Pu-T<sub>2</sub>, which can re-equilibrate to the more stable VA-Pu-T<sub>1</sub> isomer in the ground state.

## Methods and Materials

### *Extraction, purification and characterization of vulpinic acid*

Letharia vulpina was collected from the bark of Douglas fir trees at Yuba Pass (Yuba Pass, CA, 39°37'03"N 120°29'24"W, elevation: ~6,700 ft). Vulpinic acid was readily extractable from Letharia vulpina thallus with 100% methanol. Large-scale extraction was done by repeated overnight extractions of dry, ground sample in the solvent with continuous stirring. Extracts were combined and concentrated in rotary evaporator. The residue was dissolved in dichloromethane (DCM) and filtered through Whatman

Grade 2 filter paper. The filtrate was partitioned through silica plug by subsequent elution with DCM and MeOH until individual fractions ran colorless. The DCM fraction was dark olive green in color and contained vulpinic acid. This fraction was dried *in vacuo* at room temperature. Vulpinic acid was recrystallized from this fraction using 3:4 ethyl acetate:hexane mixed solvent to yield chartreuse yellow crystals. Two recrystallizations yielded 4.724 g purified vulpinic acid from 100 g dry biomass. Identity of the compound was confirmed by <sup>1</sup>HNMR (Agilent PremiumCompact+ 500 MHz), single crystal X-ray diffraction (100(±1) K on a Bruker SMART APEX CCD diffractometer with Mo K $\alpha$  radiation,  $\lambda = 0.71073 \text{ \AA}$ ) and mass spectrometry (Agilent 1200 HPLC with DAD coupled to Agilent 6230 TOF mass spectrometer;  $m/z = 323.0924$ ), all of which conformed to previously published reports of characterization (SI).

### *UV-Vis and FTIR Photodegradation*

Thin films of isolated vulpinic acid (VA) were prepared by dissolving VA in acetone, depositing the solution on a quartz plate, and allowing the solvent to evaporate. The maximum optical density at 400 nm of all films were kept to approximately 0.2 OD to ensure that optical density measurements remained within the linear regime.

To prepare films of VA in  $\beta$ -cyclodextrin ( $\beta$ -CD), VA molecules were first encapsulated in  $\beta$ -CD. Encapsulation was achieved by dissolving  $\beta$ -CD and VA in d<sub>6</sub>-DMSO maintaining a 12.12 mM  $\beta$ -CD concentration and 1:1 stoichiometry with a slight excess of VA. The solution was stirred for a total of 72 hours, the first 5 hours being at 65-80 °C and the remaining 67 hours being at room temperature. The solvent was evaporated on a lyophilizer. Encapsulation of VA in  $\beta$ -CD was confirmed by <sup>1</sup>HNMR spectroscopy with significant change in chemical shifts of VA aromatic resonances following previously published method.<sup>42</sup> The FTIR absorption bands of VA also changed upon encapsulation. A thin film of

the encapsulated VA was then prepared in a similar manner to the isolated compound using water as the solvent.

VA-pullulan films were prepared by first dry-grinding VA crystals and pullulan granules in a mortar to get a powder mixture (1:10 VA:pullulan, w/w). This mixture was then wet-ground in deionized water (1:20 pullulan:water, w/w). Pullulan readily forms a viscous solution in water at this concentration. VA particles appear to be well dispersed in this solution when visualized under 10x magnification. This solution was then deposited on a quartz plate and briefly placed in a 100°C oven to facilitate the removal of water.

The films were irradiated with 400 nm light, which was generated by frequency-doubling the 800 nm output of a Ti:sapphire laser (pulse width 100 fs, repetition rate 1 kHz). The energy of each pulse was on the order of 30  $\mu$ J and the irradiated area was approximately 3 cm<sup>2</sup>. These parameters make the irradiation intensity significantly higher than what would be found in a natural environment, which serves to reduce the total time needed to observe the photodegradation of the sample. Throughout the irradiation process, spectra of the films were collected on a PerkinElmer Lambda 25 UV-Vis spectrophotometer.

Films of isolated VA and VA in pullulan were prepared for FTIR photodegradation experiments in a similar manner. CaF<sub>2</sub> plates were used as the substrate and the maximum optical density between 1500-1800 cm<sup>-1</sup> was approximately 80 mOD. Irradiation of the films was carried out using the same setup as in the UV-Vis experiments, and FTIR spectra were collected periodically with a nitrogen-purged Nicolet 6700 spectrometer.

### *Transient Absorption Spectroscopy*

Visible-pump IR-probe transient absorption spectra of isolated VA and VA in pullulan were collected by utilizing a 400 nm pump (1-7  $\mu$ J per pulse) and a broadband IR probe spanning approximately 1500-1750 cm<sup>-1</sup>. This broadband IR pulse with center wavelength 6203 nm was generated by directing a portion of the 800 nm output (~100 fs pulsedwidth) of a Ti:sapphire laser into an optical parametric amplifier and

converted to the mid-IR via difference frequency generation. The delay between the pump and probe pulses was controlled by moving a retroreflector in the pump beam path with a motorized nanomover stage. The transmitted probe pulse was focused onto the focal plane of a monochromator equipped with a 64-element mercury-cadmium-telluride array detector (InfraRed Associates, Stuart, FL). The monochromator (focal length 270 mm) used a 50 lines per mm groove grating. Picosecond time dependent spectra were obtained by sampling the frequency spectra (averaged over 3-5 scans, 900 shots per scan) at various time points from 0 ps to 25 ps and at additional timepoints of 1, 2, and 3 ns. The VA films were prepared similarly to the FTIR experiments but were made thicker in order to increase the transient absorption signal. Several time-delay scans were collected and averaged for each sample.

### *Computational details*

Equilibrium ground state geometries and Hessians of four isomers of vulpinic acid namely **VA-T<sub>1</sub>**, **VA-T<sub>2</sub>**, their Z-isomers **VA-T<sub>1z</sub>** and **VA-T<sub>2z</sub>**, as well as the 1,3-dicarbonyl tautomer (VA-CT) were computed at B3LYP/def2-SVPD level of density functional theory (DFT) (Figure S6). Additionally, we investigated the properties of the **VA-T<sub>1</sub>** and **VA-T<sub>2</sub>** isomers coordinated with methanol molecules to simulate a H-bonding network. Excited state absorption spectra, equilibrium geometries and Hessians were calculated with the time-dependent density functional theory (TD-DFT) using the same density functional and basis set. All optimized geometries exhibit absence of imaginary frequencies, except for the first excited state of the **VA-T<sub>1</sub>•2MeOH** isomer with one small imaginary frequency of 14*i* cm<sup>-1</sup>. The calculated frequencies are adjusted with an anharmonicity scaling factor of 0.964. The calculations were performed in the gas phase with the Q-Chem 5.0 electronic structure program package.<sup>43</sup> A vibrational mode decomposition analysis of the calculated IR spectra is performed using the VibAnalysis code.<sup>44</sup> Due to the current lack of interface between VibAnalysis and Q-Chem, vibrational frequencies for selected isomers are recalculated with the ORCA 5.0 program package at the same level of theory.<sup>45</sup>

## Acknowledgements

The published results are based upon work supported by the National Aeronautics and Space Administration under Grant #: 80NSSC22K1633 issued through the NASA Science Mission Directorate. T.M. was supported by a Hitchcock Center for Chemical Ecology Graduate Fellowship. The authors also thank Dr. Maksym Fizer for fruitful discussions and comments. Megan Burroughs performed the single-crystal X-ray diffraction characterization of vulpinic acid.

## References

- (1) Solovchenko, A. *Photoprotection in Plants: Optical Screening-based Mechanisms*; Springer Science & Business Media, 2010.
- (2) Baker, L. A.; Marchetti, B.; Karsili, T. N. V.; Stavros, V. G.; Ashfold, M. N. R. Photoprotection: extending lessons learned from studying natural sunscreens to the design of artificial sunscreen constituents. *Chemical Society Reviews* **2017**, *46* (12), 3770-3791, 10.1039/C7CS00102A. DOI: 10.1039/C7CS00102A.
- (3) Solhaug, K. A.; Gauslaa, Y. Secondary Lichen Compounds as Protection Against Excess Solar Radiation and Herbivores. In *Progress in Botany* 73, Lüttege, U., Beyschlag, W., Büdel, B., Francis, D. Eds.; Springer, 2012; pp 283-304.
- (4) Nguyen, K.-H.; Chollet-Krugler, M.; Gouault, N.; Tomasi, S. UV-protectant metabolites from lichens and their symbiotic partners. *Natural Product Reports* **2013**, *30* (12), 1490-1508. DOI: 10.1039/C3NP70064J (acccesed 2024-06-17 11:55:52).pubs.rsc.org.
- (5) de Vera, J.-P. Lichens as survivors in space and on Mars. *Fungal Ecology* **2012**, *5* (4), 472-479. DOI: 10.1016/j.funeco.2012.01.008 (acccesed 2024-06-17 12:12:33).ScienceDirect.
- (6) Meeßen, J.; Sánchez, F. J.; Sadowsky, A.; de la Torre, R.; Ott, S.; de Vera, J.-P. Extremotolerance and Resistance of Lichens: Comparative Studies on Five Species Used in Astrobiological Research II. Secondary Lichen Compounds. *Origins of Life and Evolution of Biospheres* **2013**, *43* (6), 501-526. DOI: 10.1007/s11084-013-9348-z (acccesed 2024-06-17 12:14:29).Springer Link.
- (7) Noetzel, R. d. I. T.; Sancho, L. G. Lichens as Astrobiological Models: Experiments to Fathom the Limits of Life in Extraterrestrial Environments. In *Extremophiles as Astrobiological Models*, John Wiley & Sons, Ltd, 2020; pp 197-220.
- (8) Honegger, R. Functional Aspects of the Lichen Symbiosis. *Annual Review of Plant Biology* **1991**, *42* (Volume 42, 1991), 553-578. DOI: 10.1146/annurev.pp.42.060191.003005 (acccesed 2024-06-17 12:30:46).[www.annualreviews.org](http://www.annualreviews.org).
- (9) Spribille, T.; Tagirdzhanova, G.; Goyette, S.; Tuovinen, V.; Case, R.; Zandberg, W. F. 3D biofilms: in search of the polysaccharides holding together lichen symbioses. *FEMS Microbiology Letters* **2020**, *367* (5), fnaa023. DOI: 10.1093/femsle/fnaa023 (acccesed 2024-06-17 12:44:55).Silverchair.
- (10) Gasulla, F.; del Campo, E. M.; Casano, L. M.; Guéra, A. Advances in Understanding of Desiccation Tolerance of Lichens and Lichen-Forming Algae. *Plants* **2021**, *10* (4), 807. DOI: 10.3390/plants10040807 (acccesed 2024-06-17 13:09:39).[www.mdpi.com](http://www.mdpi.com).
- (11) Röttger, K.; Marroux, H. J. B.; Grubb, M. P.; Coulter, P. M.; Böhnke, H.; Henderson, A. S.; Galan, M. C.; Temps, F.; Orr-Ewing, A. J.; Roberts, G. M. Ultraviolet Absorption Induces Hydrogen-Atom

- Transfer in G·C Watson–Crick DNA Base Pairs in Solution. *Angewandte Chemie International Edition* **2015**, *54* (49), 14719–14722. DOI: 10.1002/anie.201506940 (acccesed 2020/05/20).
- (12) Sauri, V.; Gobbo, J. P.; Serrano-Pérez, J. J.; Lundberg, M.; Coto, P. B.; Serrano-Andrés, L.; Borin, A. C.; Lindh, R.; Merchán, M.; Roca-Sanjuán, D. Proton/Hydrogen Transfer Mechanisms in the Guanine–Cytosine Base Pair: Photostability and Tautomerism. *Journal of Chemical Theory and Computation* **2013**, *9* (1), 481–496. DOI: 10.1021/ct3006166 (acccesed 2024-06-17 13:50:53).ACS Publications.
- (13) Phinney, N. H.; Gauslaa, Y.; Solhaug, K. A. Why chartreuse? The pigment vulpinic acid screens blue light in the lichen *Letharia vulpina*. *Planta* **2019**, *249* (3), 709–718. DOI: 10.1007/s00425-018-3034-3.
- (14) Legouin, B.; Lohézic-Le Dévéhat, F.; Ferron, S.; Rouaud, I.; Le Pogam, P.; Cornevin, L.; Bertrand, M.; Boustie, J. Specialized Metabolites of the Lichen *Vulpicida pinastri* Act as Photoprotective Agents. *Molecules* **2017**, *22* (7), 1162. DOI: 10.3390/molecules22071162 (acccesed 2024-06-17 21:46:18).[www.mdpi.com](http://www.mdpi.com).
- (15) Varol, M.; Türk, A.; Candan, M.; Tay, T.; Koparal, A. T. Photoprotective Activity of Vulpinic and Gyrophoric Acids Toward Ultraviolet B-Induced Damage in Human Keratinocytes. *Phytother Res* **2016**, *30* (1), 9–15. DOI: <https://doi.org/10.1002/ptr.5493> (acccesed 2024/06/27).
- (16) Ndlebe, V. J.; Brown, M. E.; Glass, B. D. Photostability of triprolidine hydrochloride and its mixtures with cyclodextrin and glucose. *Journal of Thermal Analysis and Calorimetry* **2004**, *77* (2), 459–470. DOI: 10.1023/B:JTAN.0000038986.03503.a6.
- (17) Scalia, S.; Casolari, A.; Iaconinoto, A.; Simeoni, S. Comparative studies of the influence of cyclodextrins on the stability of the sunscreen agent, 2-ethylhexyl-p-methoxycinnamate. *Journal of Pharmaceutical and Biomedical Analysis* **2002**, *30* (4), 1181–1189. DOI: [https://doi.org/10.1016/S0731-7085\(02\)00433-8](https://doi.org/10.1016/S0731-7085(02)00433-8).
- (18) Scalia, S.; Villani, S.; Casolari, A. Inclusion Complexation of the Sunscreen Agent 2-Ethylhexyl-p-dimethylaminobenzoate with Hydroxypropyl-β-cyclodextrin: Effect on Photostability. *Journal of Pharmacy and Pharmacology* **1999**, *51* (12), 1367–1374. DOI: <https://doi.org/10.1211/0022357991777182> (acccesed 2024/06/27).
- (19) Kockler, J.; Oelgemöller, M.; Robertson, S.; Glass, B. D. Photostability of sunscreens. *Journal of Photochemistry and Photobiology C: Photochemistry Reviews* **2012**, *13* (1), 91–110. DOI: <https://doi.org/10.1016/j.jphotochemrev.2011.12.001>.
- (20) Chai, S.; Zhao, G.-J.; Song, P.; Yang, S.-Q.; Liu, J.-Y.; Han, K.-L. Reconsideration of the excited-state double proton transfer (ESDPT) in 2-aminopyridine/acid systems: role of the intermolecular hydrogen bonding in excited states. *Physical Chemistry Chemical Physics* **2009**, *11* (21), 4385–4390, 10.1039/B816589K. DOI: 10.1039/B816589K.
- (21) Chung, K.-Y.; Chen, Y.-H.; Chen, Y.-T.; Hsu, Y.-H.; Shen, J.-Y.; Chen, C.-L.; Chen, Y.-A.; Chou, P.-T. The Excited-State Triple Proton Transfer Reaction of 2,6-Diazaindoles and 2,6-Diazatryptophan in Aqueous Solution. *Journal of the American Chemical Society* **2017**, *139* (18), 6396–6402. DOI: 10.1021/jacs.7b01672.
- (22) Abiola, T. T.; Rioux, B.; Johal, S.; Mention, M. M.; Brunissen, F.; Woolley, J. M.; Allais, F.; Stavros, V. G. Insight into the Photodynamics of Photostabilizer Molecules. *The Journal of Physical Chemistry A* **2022**, *126* (45), 8388–8397.
- (23) Rodrigues, N. D. N.; Staniforth, M.; Stavros, V. G. Photophysics of sunscreen molecules in the gas phase: a stepwise approach towards understanding and developing next-generation sunscreens. *Proceedings of the Royal Society A: Mathematical, Physical and Engineering Sciences* **2016**, *472* (2195), 20160677.
- (24) Li, C.-X.; Guo, W.-W.; Xie, B.-B.; Cui, G. Photodynamics of oxybenzone sunscreen: Nonadiabatic dynamics simulations. *The Journal of Chemical Physics* **2016**, *145* (7).

- (25) Chan, C. T.-L.; Ma, C.; Chan, R. C.-T.; Ou, H.-M.; Xie, H.-X.; Wong, A. K.-W.; Wang, M.-L.; Kwok, W.-M. A long lasting sunscreen controversy of 4-aminobenzoic acid and 4-dimethylaminobenzaldehyde derivatives resolved by ultrafast spectroscopy combined with density functional theoretical study. *Physical Chemistry Chemical Physics* **2020**, *22* (15), 8006-8020.
- (26) van der Loop, T. H.; Ruesink, F.; Amirjalayer, S.; Sanders, H. J.; Buma, W. J.; Woutersen, S. Unraveling the Mechanism of a Reversible Photoactivated Molecular Proton Crane. *The Journal of Physical Chemistry B* **2014**, *118* (45), 12965-12971. DOI: 10.1021/jp508911v.
- (27) Chevalier, K.; Wolf, M. M. N.; Funk, A.; Andres, M.; Gerhards, M.; Diller, R. Transient IR spectroscopy and ab initio calculations on ESIPT in 3-hydroxyflavone solvated in acetonitrile. *Physical Chemistry Chemical Physics* **2012**, *14* (43), 15007-15020, 10.1039/C2CP41077J. DOI: 10.1039/C2CP41077J.
- (28) Berenbeim, J. A.; Boldissar, S.; Owens, S.; Haggmark, M. R.; Gate, G.; Siouri, F. M.; Cohen, T.; Rode, M. F.; Patterson, C. S.; de Vries, M. S. Excited state intramolecular proton transfer in hydroxyanthraquinones: Toward predicting fading of organic red colorants in art. *Science Advances* **5** (9), eaaw5227. DOI: 10.1126/sciadv.aaw5227 (acccesed 2024/06/27).
- (29) Tan, J. A.; Garakyaraghi, S.; Tagami, K. A.; Frano, K. A.; Crockett, H. M.; Ogata, A. F.; Patterson, J. D.; Wustholz, K. L. Contributions from Excited-State Proton and Electron Transfer to the Blinking and Photobleaching Dynamics of Alizarin and Purpurin. *The Journal of Physical Chemistry C* **2017**, *121* (1), 97-106. DOI: 10.1021/acs.jpcc.6b09818.
- (30) Miliani, C.; Monico, L.; Melo, M. J.; Fantacci, S.; Angelin, E. M.; Romani, A.; Janssens, K. Photochemistry of Artists' Dyes and Pigments: Towards Better Understanding and Prevention of Colour Change in Works of Art. *Angewandte Chemie International Edition* **2018**, *57* (25), 7324-7334. DOI: <https://doi.org/10.1002/anie.201802801> (acccesed 2024/06/27).
- (31) Flom, S. R.; Barbara, P. F. Proton transfer and hydrogen bonding in the internal conversion of S1 anthraquinones. *The Journal of Physical Chemistry* **1985**, *89* (21), 4489-4494.
- (32) Baker, L. A.; Horbury, M. D.; Greenough, S. E.; Coulter, P. M.; Karsili, T. N. V.; Roberts, G. M.; Orr-Ewing, A. J.; Ashfold, M. N. R.; Stavros, V. G. Probing the Ultrafast Energy Dissipation Mechanism of the Sunscreen Oxybenzone after UVA Irradiation. *The Journal of Physical Chemistry Letters* **2015**, *6* (8), 1363-1368. DOI: 10.1021/acs.jpclett.5b00417.
- (33) Abid, A. R.; Marciniak, B.; Pędziński, T.; Shahid, M. Photo-stability and photo-sensitizing characterization of selected sunscreens' ingredients. *Journal of Photochemistry and Photobiology A: Chemistry* **2017**, *332*, 241-250. DOI: <https://doi.org/10.1016/j.jphotochem.2016.08.036>.
- (34) Tarras-Wahlberg, N.; Rosén, A.; Stenhagen, G.; Larkö, O.; Wennberg, A.-M.; Wennerström, O. Changes in Ultraviolet Absorption of Sunscreens After Ultraviolet Irradiation. *Journal of Investigative Dermatology* **1999**, *113* (4), 547-553. DOI: 10.1046/j.1523-1747.1999.00721.x (acccesed 2024/06/27).
- (35) Berenbeim, J. A.; Wong, N. G. K.; Cockett, M. C. R.; Berden, G.; Oomens, J.; Rijs, A. M.; Dessent, C. E. H. Unravelling the Keto–Enol Tautomer Dependent Photochemistry and Degradation Pathways of the Protonated UVA Filter Avobenzone. *The Journal of Physical Chemistry A* **2020**, *124* (15), 2919-2930. DOI: 10.1021/acs.jpca.0c01295.
- (36) Kwon, J. E.; Park, S. Y. Advanced Organic Optoelectronic Materials: Harnessing Excited-State Intramolecular Proton Transfer (ESIPT) Process. *Advanced Materials* **2011**, *23* (32), 3615-3642. DOI: <https://doi.org/10.1002/adma.201102046> (acccesed 2024/06/27).
- (37) Hsieh, C.-C.; Jiang, C.-M.; Chou, P.-T. Recent Experimental Advances on Excited-State Intramolecular Proton Coupled Electron Transfer Reaction. *Accounts of Chemical Research* **2010**, *43* (10), 1364-1374. DOI: 10.1021/ar1000499.
- (38) Demchenko, A. P.; Tang, K.-C.; Chou, P.-T. Excited-state proton coupled charge transfer modulated by molecular structure and media polarization. *Chemical Society Reviews* **2013**, *42* (3), 1379-1408, 10.1039/C2CS35195A. DOI: 10.1039/C2CS35195A.

- (39) Zhou, P.; Han, K. Unraveling the Detailed Mechanism of Excited-State Proton Transfer. *Accounts of Chemical Research* **2018**, *51* (7), 1681-1690. DOI: 10.1021/acs.accounts.8b00172.
- (40) Zhao, Y.; Wang, M.; Zhou, P.; Yang, S.; Liu, Y.; Yang, C.; Yang, Y. Mechanism of Fluorescence Quenching by Acylamino Twist in the Excited State for 1-(Acylamino)anthraquinones. *The Journal of Physical Chemistry A* **2018**, *122* (11), 2864-2870. DOI: 10.1021/acs.jpca.7b11675.
- (41) Joshi, H. C.; Antonov, L. Excited-State Intramolecular Proton Transfer: A Short Introductory Review. In *Molecules*, 2021; Vol. 26.
- (42) He, J.; Zheng, Z.-P.; Zhu, Q.; Guo, F.; Chen, J. Encapsulation mechanism of oxyresveratrol by  $\beta$ -cyclodextrin and hydroxypropyl- $\beta$ -cyclodextrin and computational analysis. *Molecules* **2017**, *22* (11), 1801.
- (43) Shao, Y.; Gan, Z.; Epifanovsky, E.; Gilbert, A. T. B.; Wormit, M.; Kussmann, J.; Lange, A. W.; Behn, A.; Deng, J.; Feng, X.; et al. Advances in molecular quantum chemistry contained in the Q-Chem 4 program package. *Molecular Physics* **2015**, *113* (2), 184-215. DOI: 10.1080/00268976.2014.952696 (acccesed 2024/06/27/17:03:51). From Taylor and Francis+NEJM.
- (44) Teixeira, F.; Cordeiro, M. N. D. Improving vibrational mode interpretation using bayesian regression. *Journal of Chemical Theory and Computation* **2018**, *15* (1), 456-470.
- (45) Neese, F. Software update: The ORCA program system—Version 5.0. *WIREs Computational Molecular Science* **2022**, *12* (5), e1606. DOI: 10.1002/wcms.1606 (acccesed 2024/06/27/17:05:06). From Wiley Online Library.